Proceedings of the International MultiConference of Engineers and Computer Scientists 2013 Vol I,
IMECS 2013, March 13 - 15, 2013, Hong Kong

Optoelectronic Correlator Based on HSV Color Space with Shifted Training Images for Chromatic Image Recognition

Shaoda Lin, Chulung Chen*, Chengsyuan You, and Yuezhe Li

Abstract—**This paper is based on the image displacement to find the reference function of the minimum average correlation energy. First, we transform the color image into three HSV color space components. Then, three components are rotated (from 5° to 355°, the interval is 5°) and shifted (x = -5 to x = 5, the interval is 1 pixel, y = -5 to y = 5, the interval is 1 pixel) at the same time. Finally, we compute the original components and process components by using linear correlation. Finally we obtain the minimum sidelobe energy of reference functions on the output plane.**

Index Terms—**Minimum average correlation energy, HSV color space, polychromatic pattern recognition, Mach-Zehnder joint transform correlator**

I. Introduction

The benefits of light are fast transmission speed, high-speed capability for parallel computing and real-time processing. In 1964, VanderLugt proposed matching spatial filter, also called VanderLugt correlator (VLC) [1]. In 1966 Weaver and Goodman [2] proposed the joint transform correlator (JTC). Compared with the VLC, the optical structure is less complicated. The target image and reference image are exhibited side by side at input plane without accurate problem. There is the energy of zero-order term in the JTC structure. It will influence the detected signal exactness. In 1995, Lu [3] removed the zero-order term with a joint transform power spectrum (JTPS) to yield the nonzero-order JTC (N0JTC) [4-6]. We can obtain high correlator peak intensity and small sidelobe energy. In 2002, Cheng et al. [7] proposed a better method that used a Mach-Zehnder based NOJTC (MZJTC), which could remove the zero order term immediately in one step. Chen et al. [8] utilized minimum average correlator energy (MACE) [9] based on Lagrange multiplier to obtain the reference function. It can yield sharper correlator peak. In order to find a better reference function, we apply this method with the displacement in training images.

In this paper, we use the HSV color space for optical pattern recognition with MZJTC. The MACE technique is also applied to devise the reference functions in the input spatial domain of the MZJTC. We adopt image displacement to find the reference function for the minimum average correlation energy in MZJTC structure.

Manuscript received August 2 2013. This work was supported by the National Science Council in Taiwan, under grants NSC100-2221-E-155-044 and NSC 101-2221-E-155 -053

Shaoda Lin is with the department of Photonics Engineering, Yuan Ze university, 135 Yung Tung Road, Taoyuan 32026, Taiwan.

Chulung Chen is with the Department of Photonics Engineering, Yuan Ze university, 135 Yung Tung Road, Taoyuan 32026, Taiwan. (Corresponding author: phone: +886-3-4638800 ext 7513; fax: +886-3-4639355; e-mail: chulung@saturn.yzu.edu.tw).

Chengsyuan You is with the Department of Photonics Engineering, Yuan Ze university, 135 Yung Tung Road, Taoyuan 32026, Taiwan.

Yuezhe Li is with the Department of Photonics Engineering, Yuan Ze university, 135 Yung Tung Road, Taoyuan 32026, Taiwan.

II. Analysis

Fig. 1 shows HSV color model. HSV color model is constructed by hue, saturation and value. Hue denotes different pure color corresponding to each angle in color plane. For example, 0°, 60°, 120°, 180°, 240°, and 300° correspond to red, yellow, green, cyan, blue and magenta, respectively. Saturation means the purity degree of a color. It mixes pure color with white light. Value is normalized from 0 to 1 to represent black and white, respectively. Value controls brightness of a color.

$$h = \begin{cases} \dfrac{\theta}{2\pi} & if \ \ \mathrm{b} \le \mathrm{g} \\ \dfrac{2\pi-\theta}{2\pi} & if \ \ \mathrm{b} > \mathrm{g} \end{cases}$$

$$\theta = \cos^{-1}\left\{ \frac{\frac{1}{2}[(r-g)+(r-b)]}{\sqrt{(r-g)^2+(r-b)(g-b)}} \right\},$$

(1)

$$s = \frac{\max(r,g,b)-\min(r,g,b)}{\max(r,g,b)}, \tag{2}$$

()1

and

$$v = \max(r,g,b). \tag{3}$$

Here max and min operators choose the maximum and minimum values of the operand, respectively. We can see that the transformation from RGB to HSV is a non-linear operation. Next, these three components will be applied in the MZJTC system.

ISBN: 978-988-19251-8-3
ISSN: 2078-0958 (Print); ISSN: 2078-0966 (Online)

Fig. 1 shows the MZJTC structure, The system is composed of an illuminant of laser, one spatial filter, one collimated lens (CL), three half wave plates (HWP), three quarter wave plates (QWP), three image capture devices (CCD1, 2, 3) cameras, three polarizing beam splitters (PBS1, 2, 3), three beam splitters (BS1, 2, 3), three Fourier lenses (FL1, 2, 3), three reflective liquid spatial light modulators (RLCSLM1, 2, 3), one electronic subtractor (ES) which is used for removing the zero-order term of JPTS, and the computer is used for commanding this system. The positions of reference and the components of target images on the input plane are expressed as follows.

$$q(x,y)=\sum_{m=1}^{3} r_m(x+d,y+z_m)+\sum_{n=1}^{3} t_n(x-d,y+z_n), \tag{4}$$

where z_1=1 , z_2=0 , z_3=-1. $q(x,y)$ means the total input scene. The target images t_n are displayed at (d,-z_m) and the reference functions r_m are displayed at (-d,-z_n) on on the RLCSLM1 and the RLCSLM2, respectively. After a collimated laser beam illuminates the beam splitter 3 (BS3) and passes through the Fourier lens, we can obtain the light fields E_1 and E_2 that include the reflected and transmitted components. The summation of spectra on CCD1 is

$$E_1(u,v)=\sum_{m=1}^{3}\tau_1\cdot R_m(u,v)\cdot\exp[j2\pi(du+z_m v)] + \sum_{n=1}^{3}\gamma_2\cdot T_m(u,v)\cdot\exp[-j2\pi(du-z_n v)]. \tag{5}$$

Similarly, the summation of spectra on CCD2 is

$$E_2(u,v)=\sum_{m=1}^{3}\gamma_1\cdot R_m(u,v)\cdot\exp[j2\pi(du+z_m v)] + \sum_{n=1}^{3}\tau_2\cdot T_m(u,v)\cdot\exp[-j2\pi(du-z_n v)].$$

(6)

Here (u,v) is the spatial frequency coordinate in the Fourier plane. $R(u,v)$ and $T(u,v)$ represent the corresponding Fourier transforms of $r(u,v)$ and $t(u,v)$. τ_1 and γ_1 denote the transmission and reflection coefficients of BS3 for light incident from RLCSLM1. τ_2 and γ_2 denote the transmission and reflection coefficients of BS3 for light incident from RLCSLM2.

The resultant irradiation on CCD1 is given by

$$\begin{aligned} I_1(u,v) &= \left|E_1(u,v)\right|^2 \\ &= \left|\tau_1\right|^2\cdot\sum_{m=1}^{3}\sum_{m'=1}^{3} R_m(u,v)R_{m'}^*(u,v)\cdot\exp\left[j2\pi\left(z_m-z_{m'}\right)v\right] \\ &+ \left|\gamma_2\right|^2\cdot\sum_{n=1}^{3}\sum_{n'=1}^{3} T_n(u,v)T_{n'}^*(u,v)\cdot\exp\left[j2\pi\left(z_n-z_{n'}\right)v\right] \\ &+ \tau_1^*\gamma_2\cdot\sum_{m=1}^{3}\sum_{n=1}^{3} R_m(u,v)T_n^*(u,v)\cdot\exp\{j2\pi[(z_m-z_n)v+2du]\} \\ &+ \tau_1\gamma_2^*\cdot\sum_{m=1}^{3}\sum_{n=1}^{3} R_m^*(u,v)T_n(u,v)\cdot\exp\{-j2\pi[(z_m-z_n)v+2du]\}. \end{aligned} \tag{7}$$

And the resultant irradiation on CCD2 is given by

$$\begin{aligned} I_2(u,v) &= \left|E_1(u,v)\right|^2 \\ &= \left|\gamma_1\right|^2\cdot\sum_{m=1}^{3}\sum_{m'=1}^{3} R_{m2}(u,v)R_{m'}^*(u,v)\cdot\exp\left[j2\pi\left(z_m-z_{m'}\right)v\right] \\ &+ \left|\tau_2\right|^2\cdot\sum_{n=1}^{3}\sum_{n'=1}^{3} T_n(u,v)T_{n'}^*(u,v)\cdot\exp\left[j2\pi\left(z_n-z_{n'}\right)v\right] \\ &+ \tau_2\gamma_1^*\cdot\sum_{m=1}^{3}\sum_{n=1}^{3} R_m(u,v)T_n^*(u,v)\cdot\exp\{j2\pi[(z_m-z_n)v+2du]\} \\ &+ \tau_2^*\gamma_1\cdot\sum_{m=1}^{3}\sum_{n=1}^{3} R_m^*(u,v)T_n(u,v)\cdot\exp\{-j2\pi[(z_m-z_n)v+2du]\}. \end{aligned}$$

(8)

Here the superscript * means the complex conjugate. In order to remove the zero-order term, we sent the outputs of CCD1 and CCD2 to the ES, the output intensity of ES is shown as

$$\begin{aligned} I_S &= \left|E_2(u,v)\right|^2-\left|E_1(u,v)\right|^2 \\ &= \left(\left|\gamma_1\right|^2-\left|\tau_1\right|^2\right)\sum_{m=1}^{3}\sum_{m'=1}^{3} R_m(u,v)R_{m'}^*(u,v)\exp\left[j2\pi\left(z_m-z_{m'}\right)v\right] \\ &+ \left(\left|\tau_2\right|^2-\left|\gamma_2\right|^2\right)\sum_{n=1}^{3}\sum_{n'=1}^{3} T_n(u,v)T_{n'}^*(u,v)\exp\left[j2\pi\left(z_n-z_{n'}\right)v\right] \\ &+ \left(\tau_2\gamma_1^*-\tau_1^*\gamma_2\right)\sum_{m=1}^{3}\sum_{n=1}^{3} R_m(u,v)T_n^*(u,v)\exp\{j2\pi[(z_m-z_n)v+2du]\} \\ &+ \left(\tau_2^*\gamma_1-\tau_1\gamma_2^*\right)\sum_{m=1}^{3}\sum_{n=1}^{3} R_m^*(u,v)T_n(u,v)\exp\{-j2\pi[(z_m-z_n)v+2du]\}. \end{aligned} \tag{9}$$

By Stokes relations, we obtain the equation

$$\gamma_2=-\gamma_1\ , \tag{10}$$

and

ISBN: 978-988-19251-8-3
ISSN: 2078-0958 (Print); ISSN: 2078-0966 (Online)

$$|\gamma_1| = |\gamma_2| \text{ and } |\tau_1| = |\tau_2| \text{ ,} \tag{11}$$

then substitute these two conditions into equation (9). We can obtain the equation as follows.

$$I_S = 2\left|\gamma_1^* \tau_2 - \tau_1^* \gamma_2\right| \cdot \sum_{m=1}^{3} \sum_{n=1}^{3} |R_m(u,v)||T_n(u,v)| \cdot \cos\left\{2\pi[(z_m - z_n)v + 2du] + \theta + \theta_{R_m}(u,v) - \theta_{T_n}(u,v)\right\}. \tag{12}$$

θ_{R_m} and θ_{T_m} are denote the phase of $|R_m(u,v)|$ and $|T_m(u,v)|$ respectively. We sent the twelfth formula (12) to RLCSLM3, and obtain the final output on CCD3 by inverse Fourier transforming (FL3), it is shown as

$$o(x,y) = \sum_{m=1}^{3} \sum_{n=1}^{3} c_{mn}(-x,-y) \otimes \delta(x + 2d, y - z_m + z_n)\exp(-j\theta) + \sum_{m=1}^{3} \sum_{n=1}^{3} c_{mn}^*(x,y) \otimes \delta(x - 2d, y + z_m - z_n)\exp(j\theta), \tag{13}$$

and

$$c_{mn}(x,y) = r_m(x,y) \circ t_n(x,y). \tag{14}$$

Here the symbols $\circ$ and $\otimes$ respectively represent the correlation and convolution operations, and $\delta(x,y)$ is the Dirac delta function.

III. SIMULATION RESULTS

We choose a colorful butterfly to be our target image, which is shown in Fig. 3. The image has 64×64 pixels. The target image is decomposed into 3 components, which are shown in Fig. 4 Then, three components are rotated (from 5^o to 355^o, the interval is 5^o) and shifted (x = -5 to x = 5 in the horizontal direction, the interval is 1 pixel, y = -5 to y = 5 in the vertical direction, the interval is 1 pixel) at the same time. Then, we obtain the reference functions for the original components and shifted components by Lagrange multipliers method, as shown in Fig 5. We find the minimum sidelobe energy after all degrees and pixels were tested, and registered the position and the corresponding reference function. Finally, we can obtain the cross-correlation with optimal reference functions on the output plane of N0JTC. One example is shown in Fig. 6. Comparison with the non-shifted training images, the sidelobe energy for shifted training images decreases by about 30%. Meanwhile, PSR value increases by nearly 15%. Fig. 7 shows the example of 3 original color training images . Fig. 8 shows the example of 3 shifted color training images .

IV. CONCLUSIONS

This paper is based on minimum average correlation energy (MACE) with the image displacement to find the reference function. This method can yield a better reference function. So we improve the ability of image identification by combining MZJTC optical structure with MACE method and shifted training image.

REFERENCES

[1] A. VanderLugt, "Signal detection by complex spatial filtering." IEEE transactions on information theory, vol. 10, 2, pp. 139-145, 1964.
[2] C. S. Weaver and J. W. Goodman, "A Ttechnique for optically convolving two functions," Appl. Opt., vol. 5, pp. 1248-1249 , 1966.
[3] G. Lu, et al., "Implementation of a non-zero-order joint-transform correlator by use of phase-shifting techniques," *Appl. Opt.*, vol. 36, pp. 470-483, 1997.
[4] F. Cheng, et al., "Removal of intra-class associations in joint transform power spectrum," Opt. Commun., vol. 99, pp. 7-12, 1993.
[5] S. Jutamulia and D. A. Gregory, "Soft blocking of the dc term in Fourier optical systems," Opt. Eng., vol. 37, pp. 49-51, 1998.
[6] G. S. Pati and K. Singh, "Illumination sensitivity of joint transform correlators using differential processing: computer simulation and experimental studies," Opt. Commun., vol. 147, pp. 26-32, 1998.
[7] C. Cheng and H. Tu, “Implementation of a nonzero-order joint transform correlator using interferometric technique,” *Opt. Rev.*, vol. 9, 2002, pp. 193-196.
[8] C. Chen and J. Fang, "Cross-correlation peak optimization on joint transform correlators," Opt. Commun., vol. 178, pp. 315-322, 2000.
[9] A. Mahalanobis, et al., "Minimum average correlation energy filters," Appl. Opt., vol. 26, pp. 3633-3640, 1987.

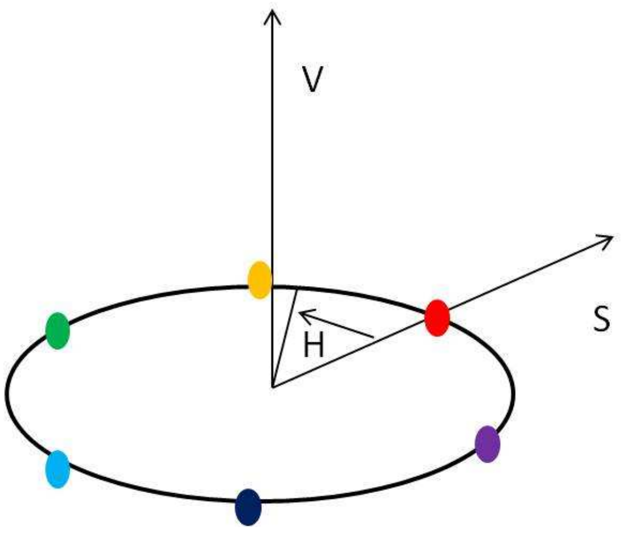

Fig. 1 HSV color model.

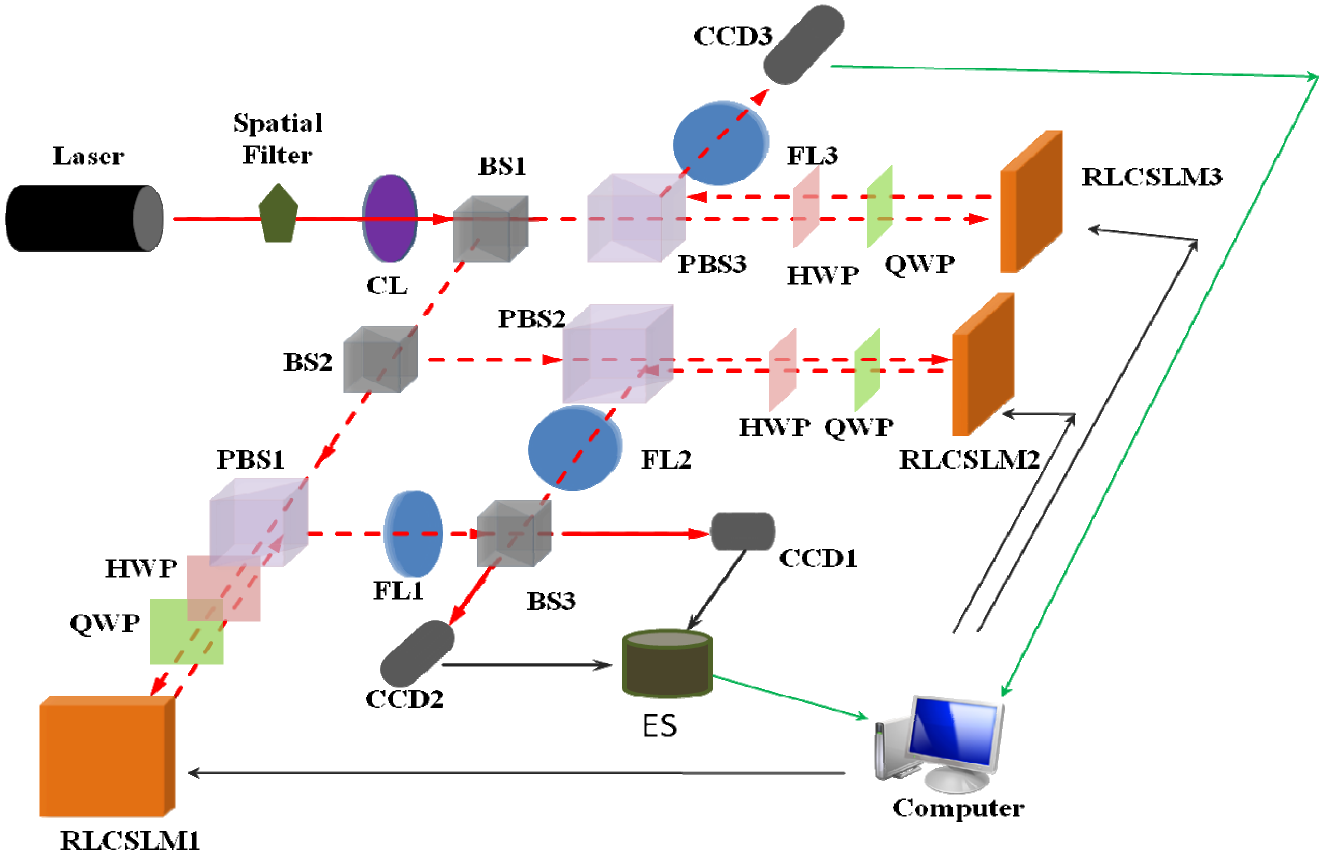

Fig. 2 Mach-Zehnder JTC structure.

Fig. 1 Target image

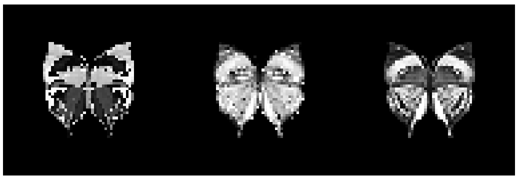

Fig. 4. Hue (left), saturation (middle), and value (right) components of target image.

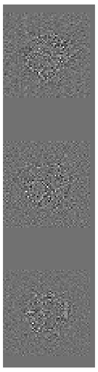

Fig. 5 Reference function yielded by simulated annealing.

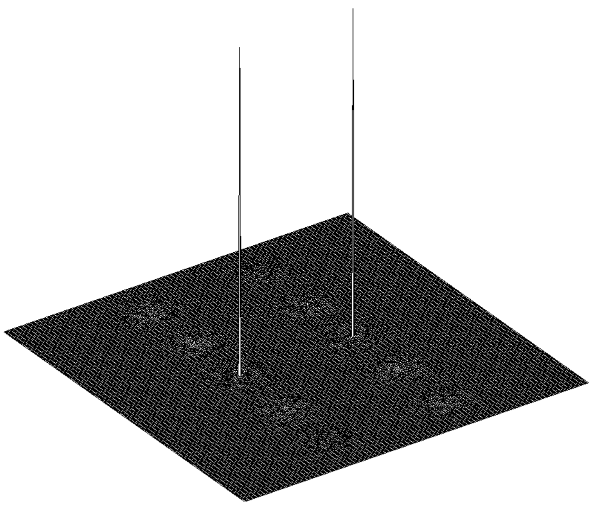

Fig. 6 Correlation output plane of NZJTC.

ISBN: 978-988-19251-8-3
ISSN: 2078-0958 (Print); ISSN: 2078-0966 (Online)

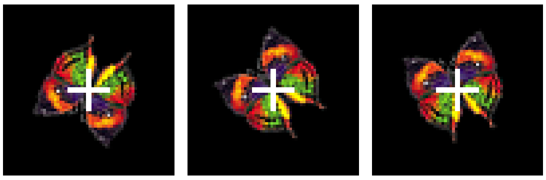

Fig.7 Some target images in the original training set.

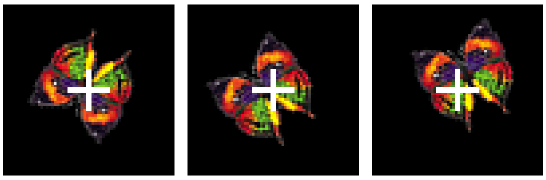

Fig.8 Corresponding images in the revised training set.

ISBN: 978-988-19251-8-3
ISSN: 2078-0958 (Print); ISSN: 2078-0966 (Online)